CHALMERS
UNIVERSITY OF TECHNOLOGY

Subspace-Based Detection in OFDM ISAC Systems Under Different Constellations

Downloaded from: https://research.chalmers.se, 2025-02-06 16:26 UTC

Citation for the original published paper (version of record):
Lai, Y., Keskin, M., Wymeersch, H. et al (2025). Subspace-Based Detection in OFDM ISAC Systems Under Different Constellations. ICASSP, IEEE International Conference on Acoustics, Speech and Signal Processing - Proceedings.
http://dx.doi.org/10.1109/ICASSP48485.2024.10446667

N.B. When citing this work, cite the original published paper.

© 2025 IEEE. Personal use of this material is permitted. Permission from IEEE must be obtained for all other uses, in any current or future media, including reprinting/republishing this material for advertising or promotional purposes, or reuse of any copyrighted component of this work in other works.

(article starts on next page)

SUBSPACE-BASED DETECTION IN OFDM ISAC SYSTEMS UNDER DIFFERENT CONSTELLATIONS

Yangming Lai[1,2], Musa Furkan Keskin[2], Henk Wymeersch[2], Luca Venturino[3], Wei Yi[1], Lingjiang Kong[1]

[1]School of Information and Communication Engineering, University of Electronic Science and Technology of China, Chengdu 611731, China
[2] Department of Electrical Engineering, Chalmers University of Technology, SE 41296 Gothenburg, Sweden
[3] Department of Electrical and Information Engineering, University of Cassino and Southern Lazio, 03043 Cassino, Italy

ABSTRACT

This paper investigates subspace-based target detection in OFDM integrated sensing and communications (ISAC) systems, considering the impact of various constellations. To meet diverse communication demands, different constellation schemes with varying modulation orders (e.g., PSK, QAM) can be employed, which in turn leads to variations in peak sidelobe levels (PSLs) within the radar functionality. These PSL fluctuations pose a significant challenge in the context of multi-target detection, particularly in scenarios where strong sidelobe masking effects manifest. To tackle this challenge, we have devised a subspace-based approach for a step-by-step target detection process, systematically eliminating interference stemming from detected targets. Simulation results corroborate the effectiveness of the proposed subspace method in achieving consistently high target detection performance under a wide range of constellation options in OFDM ISAC systems.

***Index Terms*—** Integrated sensing and communications, OFDM waveforms, constellations, subspace detection.

1. INTRODUCTION

In recent years, the popularity of integrated sensing and communications (ISAC) has surged due to the rapid expansion of spectrally co-existent radars and communication systems in 5G and advanced wireless networks [1–5]. Orthogonal frequency-division multiplexing (OFDM) waveform, which is an excellent candidate for ISAC transmission [6], has been widely studied because of its wide application in communication systems and high performance in radar detection [7–9].

This work is supported by Vinnova Grant 2021-02568.

The work of L. Venturino was supported by the European Union in the NextGenerationEU plan through the program "Bando PRIN 2022," D.D. 104/2022 (PE7, project "CIRCE," code H53D23000420006).

Generally speaking, a key step in the communication-functions realization of OFDM waveform is to employ different modulation formats (constellations) such as quadrature amplitude modulation (QAM) or phase shift keying (PSK) to modulate the data onto each subcarrier [10]. The choice of constellations depends on the communication system requirements and signal-to-noise ratio (SNR) considerations. However, it is important to note that different constellations can result in varying peak sidelobe levels (PSLs) when implementing radar functions [11, 12]. These variations can bring challenges for target detection, which is a fundamental function of the ISAC system. This is particularly true when there are significant differences in the amplitude of multiple targets, even when using windowing techniques. To the best of our knowledge, how to achieve high and consistent target detection performance for different constellation options in OFDM ISAC system has not been investigated.

In this study, we explore subspace-based target detection in OFDM ISAC systems while considering the impact of different constellations. We begin by providing a detailed overview of the OFDM ISAC system, which is capable of fulfilling both radar and communication functions through the use of various constellations. Subsequently, we introduce a subspace-based detection method designed to mitigate sidelobes from strong targets. Finally, we present a series of simulation results that showcase the effectiveness and robustness of our proposed method, particularly in achieving high and consistent target detection performance across various constellation options.

2. SYSTEM DESCRIPTION

2.1. OFDM ISAC Signal Model

We consider a monostatic OFDM ISAC system equipped with one transmitter and one radar receiver, and assume that the radar receiver has perfect knowledge of the transmitted

data [9, 13]. The complex baseband signal of an OFDM communication frame with N subcarriers and M symbols can be expressed as

$$s(t) = \frac{1}{\sqrt{N}} \sum_{m=0}^{M-1} \sum_{n=0}^{N-1} h_{n,m} e^{j2\pi n \Delta f t} \Pi \left(\frac{t - mT_{\text{sym}}}{T_{\text{sym}}} \right) \quad (1)$$

where $\Pi(t) = \begin{cases} 1, & t \in [0,1] \\ 0, & \text{otherwise} \end{cases}$ and $h_{n,m}$ represents the complex communication data symbol corresponding to the n-th subcarrier for the m-th symbol, which can belong to different constellations (e.g., PSK, QAM). Besides, T_{sym} is the total OFDM symbol duration, i.e., $T_{\text{sym}} = T_{\text{cp}} + T$ where T_{cp} and T denote the durations of the cyclic prefix (CP) and of the OFDM symbol, respectively. The subcarrier spacing and the total bandwidth are $\Delta f = 1/T$ and $B = N\Delta f = N/T$, respectively. Then the upconverted transmit signal over the block of M symbols can be represented as $\Re\left\{s(t)e^{j2\pi f_c t}\right\}$, where f_c is the carrier frequency.

We assume that there are $K \geq 1$ point-like targets with round-trip delays τ_k, Doppler shifts ν_k and complex amplitudes α_k $(k = 1, ..., K)$ in the surveillance area of the OFDM ISAC system. Then the received continuous-time passband backscattered signal can be expanded as

$$\Re\left\{ \sum_{k=1}^{K} \alpha_k s(t - \tau_k(t)) e^{j[2\pi f_c (t - \tau_k(t))]} \right\} \quad (2)$$

where $\tau_k(t) = \tau_k - \nu_k t$ is the time-varying delay. Then we can write the baseband signal by downconverting the passband signal in (2) and making the narrowband approximation $s(t - \tau_k(t)) \approx s(t - \tau_k)$ as

$$r(t) = \sum_{k=1}^{K} \alpha_k s(t - \tau_k) e^{-j2\pi f_c \tau_k} e^{j2\pi f_c \nu_k t}. \quad (3)$$

Here, we assume that the Doppler-induced phase rotation within an OFDM symbol duration is negligible, i,e, $f_c \nu_k T_{\text{sym}} \ll 1$ so that we have $f_c \nu_k t \approx f_c \nu_k m T_{\text{sym}}$. Then after removing the CP, sampling $r(t)$ at $t = mT_{\text{sym}} + T_{\text{cp}} + \ell T/N$ for $\ell = 0, \ldots, N-1, m = 0, \ldots, M-1$, and absorbing the constant term $e^{-j2\pi f_c \tau_k}$ into the target amplitude α_k, we can obtain the discrete-time domain signal for the m-th symbol as

$$\begin{aligned} r_m[\ell] = &\sum_{k=1}^{K} \alpha_k e^{j2\pi f_c m T_{\text{sym}} \nu_k} \\ &\times \frac{1}{\sqrt{N}} \sum_{n=0}^{N-1} h_{n,m} e^{j2\pi n \frac{\ell}{N}} e^{-j2\pi n \Delta f \tau_k}. \end{aligned} \quad (4)$$

Here, we denote by

$$\mathbf{b}(\tau_k) \triangleq \left[1, e^{-j2\pi \Delta f \tau_k}, \ldots, e^{-j2\pi (N-1) \Delta f \tau_k}\right]^\top \quad (5)$$

and

$$\mathbf{c}(\nu_k) \triangleq \left[1, e^{-j2\pi f_c T_{\text{sym}} \nu_k}, \ldots, e^{-j2\pi f_c (M-1) T_{\text{sym}} \nu_k}\right]^\top \quad (6)$$

the frequency-domain and temporal steering vectors, respectively. Accounting for the existence of noise, the fast-time vector for the m-th OFDM symbol is obtained as

$$\mathbf{r}_m = \sum_{k=1}^{K} \alpha_k \left(\mathbf{h}_m \odot \left(\mathbf{b}(\tau_k) [\mathbf{c}^*(\nu_k)]_m \right) \right) + \mathbf{z}_m \in \mathbb{C}^{N \times 1} \quad (7)$$

where $\mathbf{z}_m \in \mathbb{C}^{N \times 1}$ is the additive noise matrix with $\text{vec}(\mathbf{z}_m) \sim \mathcal{CN}\left(\mathbf{0}, \sigma^2 \mathbf{I}\right)$ and $\mathbf{h}_m \triangleq [h_{0,m}, \ldots, h_{N-1,m}]^\top$.

By aggregating (7) across M symbol intervals, the received OFDM ISAC signal over a frame can be expressed as

$$\mathbf{R} = \sum_{k=1}^{K} \alpha_k \left(\mathbf{H} \odot \left(\mathbf{b}(\tau_k) \mathbf{c}^H(\nu_k) \right) \right) + \mathbf{Z} \in \mathbb{C}^{N \times M}, \quad (8)$$

where $\mathbf{R}, \mathbf{H}, \mathbf{Z} \in \mathbb{C}^{N \times M}$, $\mathbf{R} \triangleq [\mathbf{r}_0, \ldots, \mathbf{r}_{M-1}]$, $\mathbf{H} \triangleq [\mathbf{h}_0, \ldots, \mathbf{h}_{M-1}]$, and $\mathbf{Z} \triangleq [\mathbf{z}_0, \ldots, \mathbf{z}_{M-1}]$.

2.2. Standard FFT-based CFAR Detector

Here we employ the standard FFT-based method in [14] to process the matrix $\mathbf{R}$ in (8) to obtain range-Doppler data planes. Then we apply the cell average constant false alarm rate (CA-CFAR) detector in [15] to detect the targets. The specific details of the standard FFT-based CFAR detector are omitted here due to space limitations of this paper.

3. SUBSPACE DETECTION METHOD

In this section, we first reorganize the received signal in a vector form and then propose a subspace-based method to mitigate sidelobes from strong targets in OFDM ISAC systems across various constellations.

3.1. The Reassembly of Received Signals

The received OFDM ISAC signal in (8) can be reassembled as follows

$$\begin{aligned} \boldsymbol{y} &\triangleq \begin{bmatrix} \mathbf{r}_0 \\ \vdots \\ \mathbf{r}_{M-1} \end{bmatrix} \in \mathbb{C}^{NM \times 1} \\ &= \begin{bmatrix} \sum_{k=1}^{K} \alpha_k \mathbf{h}_0 \odot \mathbf{b}(\tau_k) [\mathbf{c}^*(\nu_k)]_0 + \mathbf{z}_0 \\ \vdots \\ \sum_{k=1}^{K} \alpha_k \mathbf{h}_{M-1} \odot \mathbf{b}(\tau_k) [\mathbf{c}^*(\nu_k)]_{M-1} + \mathbf{z}_{M-1} \end{bmatrix} \\ &= \sum_{k=1}^{K} \alpha_k \boldsymbol{s}(\boldsymbol{x}_k) + \boldsymbol{z} \end{aligned} \quad (9)$$

where $\boldsymbol{z} \triangleq [\mathbf{z}_0^\top, \ldots, \mathbf{z}_{M-1}^\top]^\top \in \mathbb{C}^{NM\times 1}$ is a complex circularly-symmetric Gaussian vector with covariance $C_{\boldsymbol{z}} = \sigma^2\mathbf{I}$, $\boldsymbol{x}_k = (\tau_k, \nu_k)$, for $k = 1, ..., K$, which belong to an assumed inspected delay and Doppler shift points set $\mathcal{G}$, and

$$\boldsymbol{s}(\boldsymbol{x}_k) \triangleq \begin{bmatrix} \mathbf{h}_0 \odot \mathbf{b}(\tau_k)[\mathbf{c}^*(\nu_k)]_0 \\ \vdots \\ \mathbf{h}_{M-1} \odot \mathbf{b}(\tau_k)[\mathbf{c}^*(\nu_k)]_{M-1} \end{bmatrix} \in \mathbb{C}^{NM\times 1}. \tag{10}$$

3.2. A Subspace Method for Eliminating the Sidelobes of Strong Targets

From (9), it is evident that $\boldsymbol{y}$ results from the superposition of noise and an unspecified quantity of *subspace signals* originated from K targets. Leveraging the design methodologies of [16–18], we can extract one target from the received signal at each detection iteration, consider it as an additive subspace interference, and subsequently utilize an estimated interference-plus-noise covariance matrix to remove it. Therefore, we can write the following sequence of composite binary hypothesis tests as

$$\begin{aligned} \mathcal{H}_1^{(1)}: \ & \boldsymbol{y} = \boldsymbol{s}(\boldsymbol{x}^{(1)})\alpha(\boldsymbol{x}^{(1)}) + \boldsymbol{z} \\ \mathcal{H}_0^{(1)}: \ & \boldsymbol{y} = \boldsymbol{z}, \end{aligned} \tag{11}$$

if the iteration index $q = 1$ and

$$\begin{aligned} \mathcal{H}_1^{(q)}: \ & \boldsymbol{y} = \boldsymbol{s}(\boldsymbol{x}^{(q)})\alpha(\boldsymbol{x}^{(q)}) + \hat{\boldsymbol{S}}^{(q-1)}\hat{\boldsymbol{\alpha}}^{(q-1)} + \boldsymbol{z} \\ \mathcal{H}_0^{(q)}: \ & \boldsymbol{y} = \hat{\boldsymbol{S}}^{(q-1)}\hat{\boldsymbol{\alpha}}^{(q-1)} + \boldsymbol{z}, \end{aligned} \tag{12}$$

for $q \geq 2$, where $\boldsymbol{x}^{(q)}$ and $\alpha(\boldsymbol{x}^{(q)})$ are the position and amplitude of the q-th target, $\hat{\boldsymbol{S}}^{(q-1)} = [\boldsymbol{s}(\hat{\boldsymbol{x}}^{(1)}), \ldots, \boldsymbol{s}(\hat{\boldsymbol{x}}^{(q-1)})]^\top$, $\hat{\boldsymbol{\alpha}}^{(q-1)} = [\hat{\alpha}(\hat{\boldsymbol{x}}^{(1)}), \ldots, \hat{\alpha}(\hat{\boldsymbol{x}}^{(q-1)})]^\top$, and $\hat{\boldsymbol{x}}^{(1)}, ..., \hat{\boldsymbol{x}}^{(q-1)}$ are the estimated positions, the variables $\{\hat{\alpha}(\hat{\boldsymbol{x}}^{(i)})\}_{i=1}^{q-1}$ are modeled to follow a Gaussian distribution with a specific variance $\sigma^2_{\hat{\alpha}(\hat{\boldsymbol{x}}^{(i)})}$. In the following, the interference-plus-noise covariance matrix under $\mathcal{H}_0^{(q)}, \forall q$ can be written as

$$\boldsymbol{C}^{(q)} = \begin{cases} \boldsymbol{C}_{\boldsymbol{z}}, \text{ if } q = 1 \\ \sum_{i=1}^{q-1} \boldsymbol{s}\left(\hat{\boldsymbol{x}}^{(i)}\right)\sigma^2_{\hat{\alpha}(\hat{\boldsymbol{x}}^{(i)})}\boldsymbol{s}^H\left(\hat{\boldsymbol{x}}^{(i)}\right) + \boldsymbol{C}_{\boldsymbol{z}}, \text{ for } q \geq 2. \end{cases} \tag{13}$$

Then, the two negative log-likelihood functions are

$$-\ln f_0^{(q)}(\boldsymbol{y}) = \ln\left(\pi^{NM}\det \boldsymbol{C}^{(q)}\right) + \left\|\left(\boldsymbol{C}^{(q)}\right)^{-1/2}\boldsymbol{y}\right\|^2 \tag{14}$$

and

$$\begin{aligned} -\ln f_1^{(q)}(\boldsymbol{y}; \boldsymbol{x}^{(q)}, \alpha(\boldsymbol{x}^{(q)})) &= \ln\left(\pi^{NM}\det \boldsymbol{C}^{(q)}\right) \\ &+ \left\|\left(\boldsymbol{C}^{(q)}\right)^{-1/2}\left(\boldsymbol{y} - \boldsymbol{s}(\boldsymbol{x}^{(q)})\alpha(\boldsymbol{x}^{(q)})\right)\right\|^2 \end{aligned} \tag{15}$$

under $\mathcal{H}_0^{(q)}$ and $\mathcal{H}_1^{(q)}, \forall q$, respectively. Next, based on the generalized information criterion (GIC) [19, 20], we can obtain the decision rule and detailed expansions as

$$\arg\max_{\boldsymbol{x}^{(q)}\in\mathcal{G}} \mathrm{J}^{(q)}(\boldsymbol{x}^{(q)}) \underset{\mathcal{H}_0^{(q)}}{\overset{\mathcal{H}_1^{(q)}}{\gtrless}} \gamma, \tag{16}$$

where

$$\begin{aligned} \mathrm{J}^{(q)}(\boldsymbol{x}^{(q)}) &= \ln\frac{f_1^{(q)}\left(\boldsymbol{y}; \boldsymbol{x}^{(q)}, \alpha(\boldsymbol{x}^{(q)})\right)}{f_0^{(q)}\left(\boldsymbol{y}\right)} \\ &= \left\|\boldsymbol{T}^{(q)}(\boldsymbol{x}^{(q)})(\boldsymbol{C}^{(q)})^{-1/2}\boldsymbol{y}\right\|^2 \\ &= \left\|(\boldsymbol{C}^{(q)})^{-1/2}\boldsymbol{s}(\boldsymbol{x}^{(q)})\hat{\alpha}(\boldsymbol{x}^{(q)})\right\|^2, \end{aligned} \tag{17}$$

$$\begin{aligned} \boldsymbol{T}^{(q)}(\boldsymbol{x}^{(q)}) =& (\boldsymbol{C}^{(q)})^{-1/2}\boldsymbol{s}(\boldsymbol{x}^{(q)})\left\{\boldsymbol{s}^H(\boldsymbol{x}^{(q)})(\boldsymbol{C}^{(q)})^{-1}\boldsymbol{s}(\boldsymbol{x}^{(q)})\right\}^{-1} \\ & \boldsymbol{s}^H(\boldsymbol{x}^{(q)})(\boldsymbol{C}^{(q)})^{-1/2}, \end{aligned} \tag{18}$$

$$\begin{aligned} \hat{\alpha}(\boldsymbol{x}^{(q)}) = &\left(\boldsymbol{s}^H(\boldsymbol{x}^{(q)})(\boldsymbol{C}^{(q)})^{-1}\boldsymbol{s}(\boldsymbol{x}^{(q)})\right)^{-1} \\ & \boldsymbol{s}^H(\boldsymbol{x}^{(q)})(\boldsymbol{C}^{(q)})^{-1}\boldsymbol{y} \end{aligned} \tag{19}$$

is the maximum likelihood (ML) estimate of $\alpha(\boldsymbol{x}^{(q)})$, and the detection threshold γ can be set to satisfy a given probability of false alarm $\mathrm{P_{fa}}$.

If a threshold crossing occurs, a target detection is declared and the ML estimate of its position, say $\hat{\boldsymbol{x}}^{(q)}$, is recovered from the location of the maximum in (16). Simultaneously, the ML estimate of the corresponding gain vector is determined as $\hat{\alpha}(\hat{\boldsymbol{x}}^{(q)})$. The decision logic executes the test in (16) for $q = 1, 2, \ldots$ until no additional target is found. Finally, we replace the unknown variance $\sigma^2_{\hat{\alpha}(\hat{\boldsymbol{x}}^{(i)})}$ in (13) by $\sigma^2_{\hat{\alpha}(\hat{\boldsymbol{x}}^{(i)})} = \left\|\hat{\alpha}(\hat{\boldsymbol{x}}^{(i)})\right\|^2$.

4. PERFORMANCE ANALYSIS

In this simulation study, we consider an OFDM ISAC system with $f_c = 28$GHz, $B = 61.44$MHz, $\Delta f = 120$kHz, $N = 512$, $M = 1$, $T = 8.333\mu$s, $T_{\mathrm{cp}} = 1.666\mu$s, $T_{\mathrm{sym}} = 10\mu$s, and $\mathrm{P_{fa}} = 10^{-4}$. Two targets are placed at 30 m (Target 1) and 90 m (Target 2) in front of the system. The considered constellations include the BPSK, QPSK, 16QAM, 64QAM, 256QAM, and 1024QAM. We assume that Target 2 is the one of interest, the system performance is assessed in terms of its probability of detection ($\mathrm{P_d}$), $100/\mathrm{P_{fa}}$ Monte Carlo (MC) trails are used to set the detection thresholds, and the SNR of the k-th target is defined as $\mathrm{SNR}_k = |\alpha_k|^2/\sigma^2$. For comparison, we also include the performance obtained with the standard FFT-based CFAR detector and with the generalized likelihood ratio test with cleaned data (GLRT-CD) [17], which

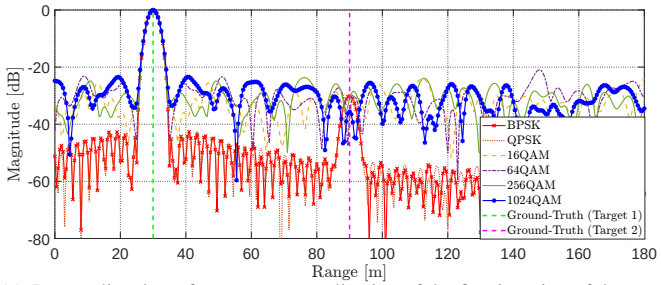

(a) Range slice data after power normalization of the first iteration of the proposed method (identical to those of the standard FFT-based method).

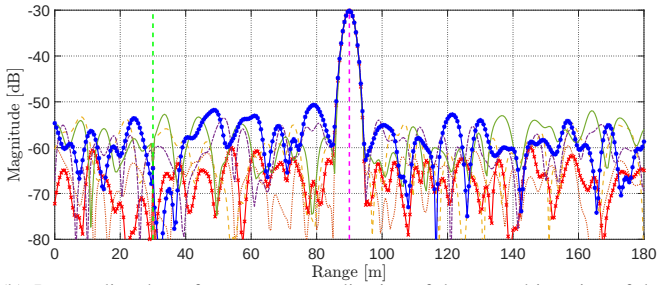

(b) Range slice data after power normalization of the second iteration of the proposed method.

Fig. 1. The range slice of the proposed subspace method and the standard FFT-based method for different constellations.

employs the proposed subspace method when the echoes produced by other targets are ideally removed, also called the single-target benchmark.

We first assume the SNRs of Targets 1 and 2 are 40 and 10 dB, and Fig. 1 shows the range slice comparison of the proposed subspace method and the standard FFT-based method employing the considered different constellation options in a single realization. It can be seen from Fig. 1(a) that the main lobes of the weak target (Target 2) are not apparent for QAM constellations due to the strong sidelobes of Target 1; obviously, it is not easy to detect Target 2 well by employing CFAR detector on this range slice for each QAM constellation. However, Fig. 1(b) shows that when employing the proposed subspace method, the sidelobes of the detected Target 1 will be removed and the main lobes of Target 2 will be apparent at the second iteration for all constellation options, thus the improvement in its detection performance is expected.

Then, we select the BPSK and 1024QAM constellations to investigate the P_d of Target 2 versus SNR_2 when $SNR_1 = 30$ dB and that versus SNR_1 when $SNR_2 = -10$ dB by MC tests. It can be seen in the top and middle figures of Fig. 2 that the standard FFT-based CFAR detector performs more badly, especially when the gap between the strong and weak targets becomes larger. However, the proposed subspace method always performs close to the GLRT-CD, showing its effectiveness and robustness in weak target detection under high sidelobes masking. Finally, the bottom figure of Fig. 2 shows the P_d of Target 2 versus different constellations

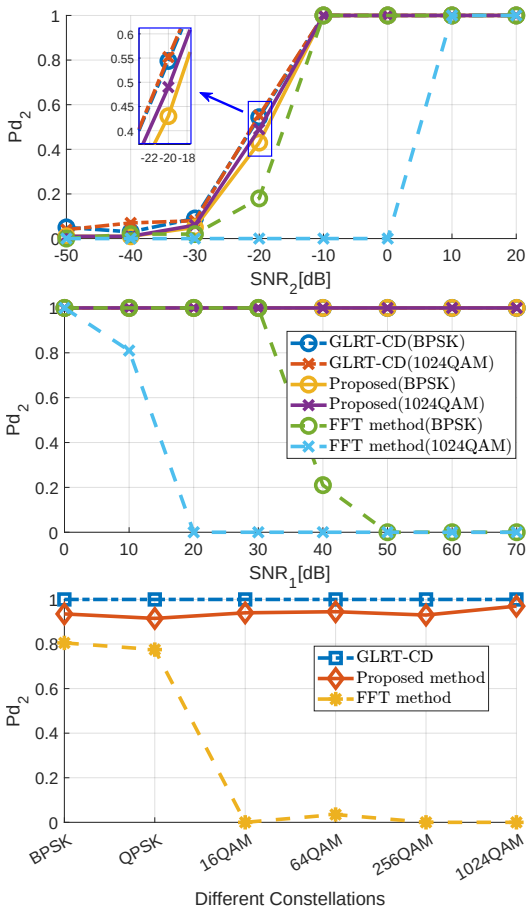

Fig. 2. P_d of Target 2 versus SNR_2 when $SNR_1 = 30$ dB (top), versus SNR_1 when $SNR_2 = -10$ dB (middle), and versus different constellations when $SNR_1 = 30$ dB and $SNR_2 = -15$ dB (bottom).

when $SNR_1 = 30$ dB and $SNR_2 = -15$ dB, we can see the proposed method achieves high and consistent target detection performance for different constellation options.

5. CONCLUSIONS

In this paper, we consider the subspace-based target detection in OFDM ISAC system under different constellations. We provided a detailed OFDM ISAC system description and derived a subspace-based procedure to gradually detect targets, upon eliminating the interference caused by the detected targets. Simulation results verified the effectiveness and robustness of the proposed subspace method. Compared to the standard FFT-based CFAR detector, the proposed method performs close to the single-target benchmark and achieve high and consistent target detection performance for different constellation options. Next, we will explore the application of the proposed subspace-based method in more intricate modulation schemes of the MIMO-OFDM ISAC systems.

6. REFERENCES

[1] Kumar Vijay Mishra, MR Bhavani Shankar, Visa Koivunen, Bjorn Ottersten, and Sergiy A Vorobyov, "Toward millimeter-wave joint radar communications: A signal processing perspective," *IEEE Signal Processing Magazine*, vol. 36, no. 5, pp. 100–114, 2019.

[2] Le Zheng, Marco Lops, Yonina C Eldar, and Xiaodong Wang, "Radar and communication coexistence: An overview: A review of recent methods," *IEEE Signal Processing Magazine*, vol. 36, no. 5, pp. 85–99, 2019.

[3] Fan Liu, Christos Masouros, Athina P Petropulu, Hugh Griffiths, and Lajos Hanzo, "Joint radar and communication design: Applications, state-of-the-art, and the road ahead," *IEEE Transactions on Communications*, vol. 68, no. 6, pp. 3834–3862, 2020.

[4] Yuanhao Cui, Fan Liu, Xiaojun Jing, and Junsheng Mu, "Integrating sensing and communications for ubiquitous iot: Applications, trends, and challenges," *IEEE Network*, vol. 35, no. 5, pp. 158–167, 2021.

[5] Fan Liu, Yuanhao Cui, Christos Masouros, Jie Xu, Tony Xiao Han, Yonina C Eldar, and Stefano Buzzi, "Integrated sensing and communications: Toward dual-functional wireless networks for 6G and beyond," *IEEE journal on selected areas in communications*, vol. 40, no. 6, pp. 1728–1767, 2022.

[6] Ebubekir Memisoglu, Talha Yłlmaz, and Hüseyin Arslan, "Waveform design with constellation extension for OFDM dual-functional radar-communications," *IEEE Transactions on Vehicular Technology*, vol. 72, no. 11, pp. 14245–14254, 2023.

[7] Fuqiang Zhang, Zenghui Zhang, Wenxian Yu, and Trieu-Kien Truong, "Joint range and velocity estimation with intrapulse and intersubcarrier doppler effects for OFDM-based radcom systems," *IEEE Transactions on Signal Processing*, vol. 68, pp. 662–675, 2020.

[8] Musa Furkan Keskin, Henk Wymeersch, and Visa Koivunen, "MIMO-OFDM joint radar-communications: Is ICI friend or foe?," *IEEE Journal of Selected Topics in Signal Processing*, vol. 15, no. 6, pp. 1393–1408, 2021.

[9] Musa Furkan Keskin, Henk Wymeersch, and Visa Koivunen, "Monostatic sensing with OFDM under phase noise: From mitigation to exploitation," *IEEE Transactions on Signal Processing*, vol. 71, pp. 1363–1378, 2023.

[10] Yong Soo Cho, Jaekwon Kim, Won Y Yang, and Chung G Kang, *MIMO-OFDM wireless communications with MATLAB*, John Wiley & Sons, 2010.

[11] Murat Temiz, Emad Alsusa, and Mohammed W Baidas, "A dual-functional massive MIMO OFDM communication and radar transmitter architecture," *IEEE Transactions on Vehicular Technology*, vol. 69, no. 12, pp. 14974–14988, 2020.

[12] Jean-Yves Baudais, Stéphane Méric, Bochra Benmeziane, and Kevin Cinglant, "Doppler robustness of joint communication and radar systems using the wiener filter," *IEEE Transactions on Communications*, vol. 71, no. 8, pp. 4807–4818, 2023.

[13] Marian Bică and Visa Koivunen, "Generalized multicarrier radar: Models and performance," *IEEE Transactions on Signal Processing*, vol. 64, no. 17, pp. 4389–4402, 2016.

[14] Klaus Martin Braun, *OFDM radar algorithms in mobile communication networks*, Ph.D. thesis, Karlsruhe, Karlsruher Institut für Technologie (KIT), Diss., 2014, 2014.

[15] Mark A Richards, *Fundamentals of radar signal processing*, vol. 1, Mcgraw-hill New York, 2005.

[16] Emanuele Grossi, Marco Lops, and Luca Venturino, "Adaptive detection and localization exploiting the ieee 802.11 ad standard," *IEEE Transactions on Wireless Communications*, vol. 19, no. 7, pp. 4394–4407, 2020.

[17] Emanuele Grossi, Marco Lops, Antonia Maria Tulino, and Luca Venturino, "Opportunistic sensing using mmwave communication signals: A subspace approach," *IEEE Transactions on Wireless Communications*, vol. 20, no. 7, pp. 4420–4434, 2021.

[18] Yangming Lai, Luca Venturino, Emanuele Grossi, and Wei Yi, "Joint detection and localization in distributed MIMO radars employing waveforms with imperfect auto- and cross-correlation," *IEEE Transactions on Vehicular Technology*, vol. 72, no. 12, pp. 16524–16537, 2023.

[19] Petre Stoica and Yngve Selen, "Model-order selection: a review of information criterion rules," *IEEE Signal Processing Magazine*, vol. 21, no. 4, pp. 36–47, 2004.

[20] Petre Stoica, Yngve Selen, and Jian Li, "On information criteria and the generalized likelihood ratio test of model order selection," *IEEE Signal Processing Letters*, vol. 11, no. 10, pp. 794–797, 2004.